

Machining strategy in five-axis milling using balance of the transversal cutting force

Patrick Gilles · Guillaume Cohen · Frederic Monies · Walter Rubio

Received: 21 May 2013 / Accepted: 2 September 2013 / Published online: 16 March 2014
© Springer-Verlag London 2014

Abstract Several solutions can be considered to resolve the problem of positioning a cutting tool on a free-form surface when five-axis milling. To choose a unique solution, in addition to the cutter–workpiece contact, an additional criterion can be taken into account. This may concern the local geometry of the surface or yet again the width milled to maximise the metal removal rate, but technological criteria relating to the cutting phenomenon and the quality of the surface produced are not considered. The present article introduces a strategy applying positioning combined with balancing of the transversal cutting force. This method involves using the ploughing effect of the milling cutters by simultaneously engaging the teeth located to the front of the cutter in relation to the feed movement and also those to the rear. The positioning obtained stabilises the cutter and contributes to making a net improvement in its dynamic behaviour. This leads in turn to significantly higher quality of the milled surface. The article presents a method to apply balancing of the transversal cutting force to two types of machining passes and elaborates an associated strategy to plan cutter paths enabling an improvement in surface quality to be achieved.

Keywords Five-axis milling · Machining strategy · Balance of the transversal cutting force · Complex-shaped workpiece

P. Gilles (✉) · G. Cohen · F. Monies · W. Rubio
Institut Clément Ader, 135 avenue de Rangueil, 31077
Toulouse cedex 4, France
e-mail: gilles@insa-toulouse.fr

G. Cohen
e-mail: guillaume.cohen@univ-tlse3.fr

F. Monies
e-mail: frederic.monies@univ-tlse3.fr

W. Rubio
e-mail: walter.rubio@univ-tlse3.fr

1 Introduction

Various methods for the management of local interference in five-axis milling position the cutter at the point considered C_c of the surface (Fig. 1). The axis of the cutter concerned is then aligned with the normal to that surface on C_c . With the cutter being positioned through consideration for a single point, a part of the cutter may come to be at the intersection with the surface. There will then be local interference (Fig. 1).

To free the cutter from the interference, an angular correction is applied to the orientation of its axis. A first major family of positioning strategies [1–4] uses the curvatures of the portion of the surface located under the cutter, but in this case, the computed solution will be unique. It will thus be impossible to take an additional criterion into account. These positioning solutions will not be given in detail here. The other big positioning family relies on calculating the distance between the cutter and the surface. In practical terms, several distances are computed between points of the cutter and the surface. These are expressed in the local reference to the surface whose origin (Fig. 1) is the point considered C_c , while \mathbf{n} is the normal vector, \mathbf{t} the vector tangent in the feed direction and \mathbf{b} the binormal vector such that $\mathbf{b} = \mathbf{n} \wedge \mathbf{t}$. The orientation of the cutter axis is computed such that these distances always remain positive so the cutter has no intersection with the surface and local interference is eliminated. Lee [5] and Fan and Ball [6] use this type of method to calculate a cutter orientation using angles taken about b and n . By the same principle, Warkentin et al. [7] and Gray et al. [8] determine the orientation of the cutter from three points of contact between the cutter and the workpiece. This is thus referred to as multi-point positioning. Adopting a different approach, Rubio [9] uses an offset surface and an equivalent cutter to calculate the positioning of a torus milling cutter on free-form surfaces determining an angle α taken about \mathbf{b} and an angle β taken about \mathbf{t} . He thus defines a domain of positioning solutions within which a particular

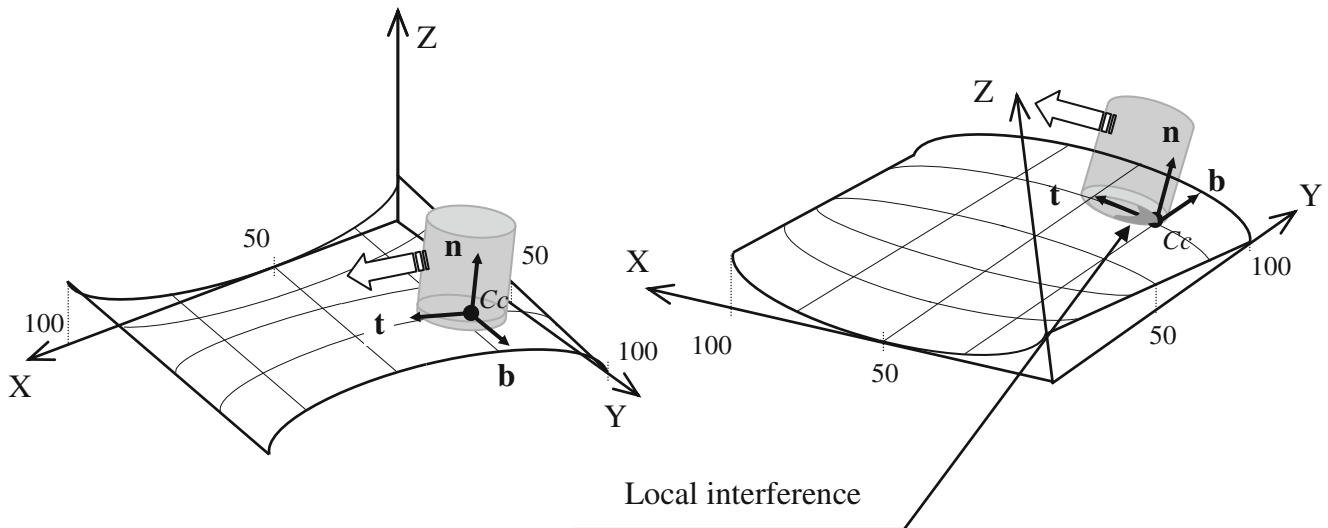


Fig. 1 Local interference

solution can be chosen through introducing an additional criterion. The torus milling cutters (Fig. 2) considered by Rubio [9] and Gilles et al. [10–13] are interesting as they combine the advantages of both cylindrical and hemispheric tools. Firstly, they admit a change in orientation (Fig. 2) by a rotation around the insert centre, then the cutting edges are kept away from the axis of rotation and the cutting speed is thus never null. Furthermore, some torus cutters with round inserts can handle ploughing (Fig. 2), meaning that the rear part of the cutter can be engaged and contribute to machining. This ploughing is defined by an angle α between the cutter axis and the normal to the surface \mathbf{n} .

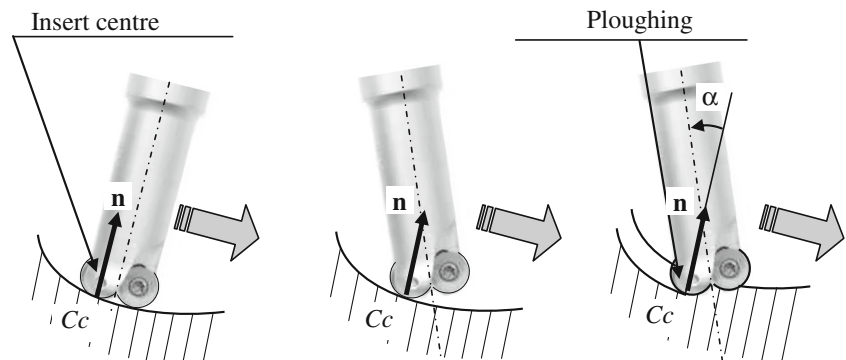
Most of the positioning methods that have just been mentioned suggest orienting the axis of the cutter with a positive tool axis inclination. Contrary to such conventional methods, Gilles et al. [13] use torus cutters with a negative rearward inclination, meaning in a ploughing situation (Fig. 2) to define a positioning that is an adaptation of that used by a number of authors (Redonnet et al., Monies et al., and also Gilles et al. [14–16]). As with Rubio [9], this relies on computing the distances d_i (Fig. 3) between points M_i of the cutter and the surface to be machined and requires that they must remain positive.

To each point M_i , there correspond a relation $\beta_i = \text{function}(\alpha_i)$ and a curve (Fig. 4). A domain of solutions is highlighted. In their works, Gilles et al. [13] choose a solution that integrates “balance of the transversal cutting force”: the minimum angle α_{mini} defined by Monies [15] that eliminates local interference is increased by the value of the balance angle α_{eq} whose determination is recalled in Section 2.1.1. The angle β retained is that whose absolute value is minimal in order to limit angular displacement during passes and thus produces a smoothing effect.

This method [13] improves the dynamic behaviour of the cutter [12] and allows better surface quality to be obtained. It uses an additional criterion considering the cutting force. However, these previous works are limited to local positioning of the cutter on the surface and the case of full slotting.

In what follows, the transversal cutting force balance principle will be recalled for the case of full slotting, and balancing of rework passes centred between two passes executed in full slotting will be defined. A complete machining strategy using these two types of passes will then be devised, and experimental validation will show the gains obtained in terms of roughness—thanks to this new strategy.

Fig. 2 Change in orientation of a torus milling cutter and ploughing



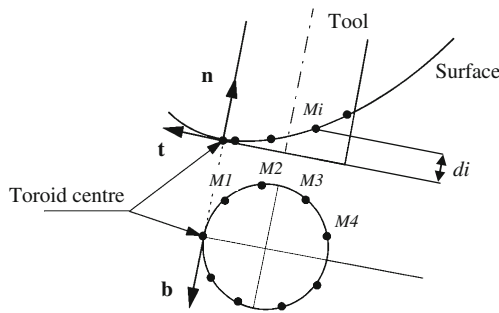


Fig. 3 Characteristic points according to Rubio [9]

2 Machining strategy associated with torus cutter positioning using balance of the transversal cutting force

2.1 Balance of the transversal cutting force

2.1.1 Reminder of the balance principle: case of full slotting

The model for the initial cutting force is defined by its components Ft, Fr and Fa (Fig. 5). Ft is the tangential force, Fr the radial force and Fa the axial force defined as follows:

$$F_t(\theta) = K_t(\theta) \times S(\theta) = K_t(\theta) \cdot d_a \cdot f_t \cdot \sin(\theta) \tag{1}$$

$$F_r(\theta) = K_r \cdot F_t(\theta) \tag{2}$$

$$F_a(\theta) = K_a \times F_t(\theta) \tag{3}$$

In these expressions, $S(\theta)$ is the chip cross-section instantaneously seen by the insert, f_t is the feed per tooth and d_a the axial engagement. The two coefficients K_r and K_a are constants. Coefficient $K_t(\theta)$ depends on the mean thickness of the chip $e_{moy}(\theta)$ at position θ (Eq. 4).

$$K_t(\theta) = K_{to} \times (e_{moy}(\theta))^v \tag{4}$$

K_{to} and v are constant coefficients. For the position considered θ , the chip mean thickness (θ) is defined (Eqs. 5 and 6)

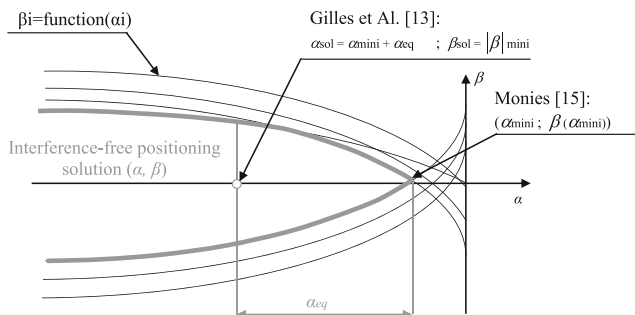


Fig. 4 Interference-free positioning with balance of the transversal cutting force

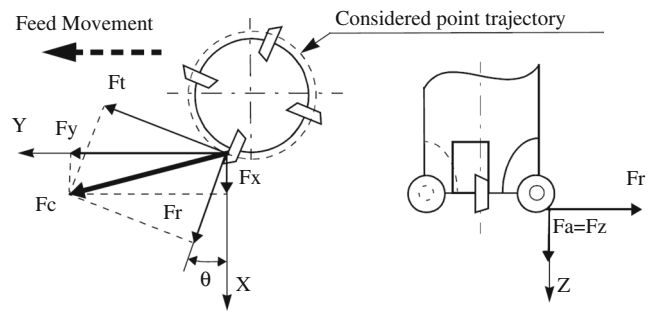


Fig. 5 Cutting force components

by Gilles et al. [10] from the feed per tooth f_t , the axial engagement d_a and the radius of the round insert R (Fig. 6).

$$e_{moy}(\theta) = \frac{1}{R \cdot \left(\frac{\pi}{2} - \phi_o\right)} \int_{\phi_o}^{\frac{\pi}{2}} f_t \cdot \sin(\theta) \cdot \cos(\phi) \cdot R d\phi = \frac{f_t \cdot \sin(\theta) \cdot d_a}{R \cdot \left(\frac{\pi}{2} - \phi_o\right)} \tag{5}$$

With

$$\phi_o = \sin^{-1} \left(\frac{(R - d_a)}{R} \right) \tag{6}$$

Gilles et al. [11] adapted the model thus defined to the ploughing situation characterised by angle α : to take into account the specific nature of the cut on the interior and exterior of the inserts, coefficient K_{to} (Eq. 4) is replaced by two coefficients K_{int} and K_{ext} and axial engagement d_a is characterised on each of these two zones using engagements $d_{a,int}(\theta)$ and $d_{a,ext}(\theta)$ calculated for each position θ (Fig. 7).

The model obtained therefore allows components Ft and Fr to be calculated and thus components Fx and Fy of the force in the fixed reference (O, X, Y, Z) defined in Fig. 5 (Eq. 7):

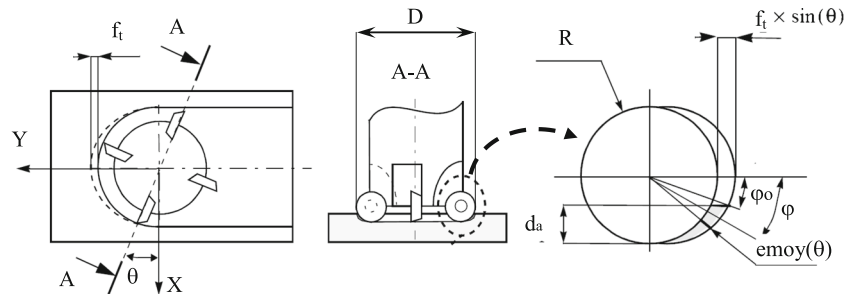
$$\begin{pmatrix} F_x(\theta) \\ F_y(\theta) \end{pmatrix} = \begin{pmatrix} \cos(\theta) & -\sin(\theta) \\ \cos(\alpha) \times \sin(\theta) & \cos(\theta) \times \cos(\alpha) \end{pmatrix} \times \begin{pmatrix} F_r(\theta) \\ F_t(\theta) \end{pmatrix} \tag{7}$$

The transversal cutting force is defined by Gilles et al. [11–13] as the cutting force component that is perpendicular to the plane formed by the direction of feed and the cutter axis. Where this feed direction is Y, this will involve a force Fx (Fig. 8). Balancing involves calculating the angle α_{eq} by equalising the absolute maximum and minimum values (Eq. 8):

$$\alpha_{eq} / \text{MAX}(F_x) = \text{MIN}(F_x) \tag{8}$$

The example given in Fig. 8 corresponds to full slotting in C35-E (standard NF EN 10083-1) with a milling cutter $D =$

Fig. 6 Mean chip thickness for round inserts



16 mm, $R=4$ mm, $d_a=2$ mm, $f_t=0.2$ mm and a cutting speed of 140 m/min. The corresponding balance angle will then be $\alpha_{eq}=-9.022^\circ$. This balancing reduces the amplitude of the F_x component and ensures improvement in the cutter’s dynamic behaviour. Works by Gilles et al. [12] show that in full slotting work, this results in a significant improvement in the surface condition.

2.1.2 Case of re-machining passes

A re-machining pass is a machining pass located in the middle of two other passes made previously in full slotting (Fig. 9) with

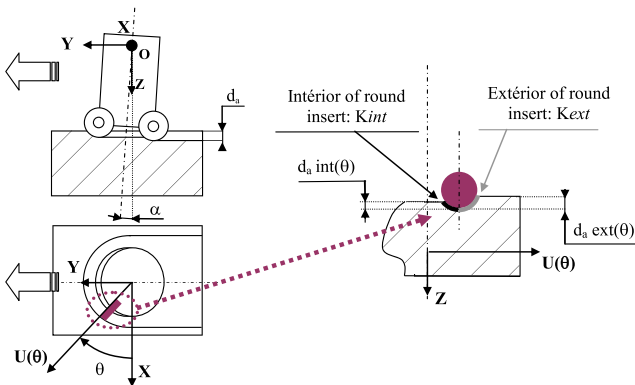


Fig. 7 Interior and exterior of inserts

the balance angle calculated in Section 2.1.1. Contact between the cutter and the workpiece occurs in accordance with the envelope curve (Fig. 9) defined by Chiou and Lee [17]:

$$\mathbf{n}_{tool} \cdot \mathbf{V} = 0 \tag{9}$$

In this expression, \mathbf{n}_{tool} is the normal to the cutter at the point considered and \mathbf{V} is the speed vector at the point considered for the cutter in relation to the workpiece.

The quantity of material a re-machining pass will remove will depend on the cutter axis inclination α . Meanwhile, the force model implemented in Section 2.1.1 requires the axial engagements $d_{a\ int}(\theta)$ and $d_{a\ ext}(\theta)$ (Fig. 7) to be known. These depend in turn on the angle α sought: the problem is thus recursive and will be resolved in what follows iteratively in two stages. This means a re-machining pass is performed with a cutter axis inclination α (Fig. 10) to the rear of the cutter. The surface S_{sup} is milled by the front of the cutter, mainly by the exterior of the insert (Fig. 10). Then, similarly, the surface S_{inf} is removed by the rear of the cutter with the interior of the insert.

- First stage: An angle α_{rinit} is computed (Eq. 10) by equalising the axial engagement of the front and the rear of the cutter (Fig. 10):

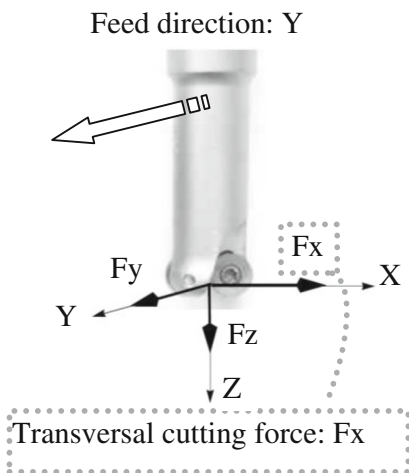


Fig. 8 Balance of the transverse cutting force F_x in full slotting

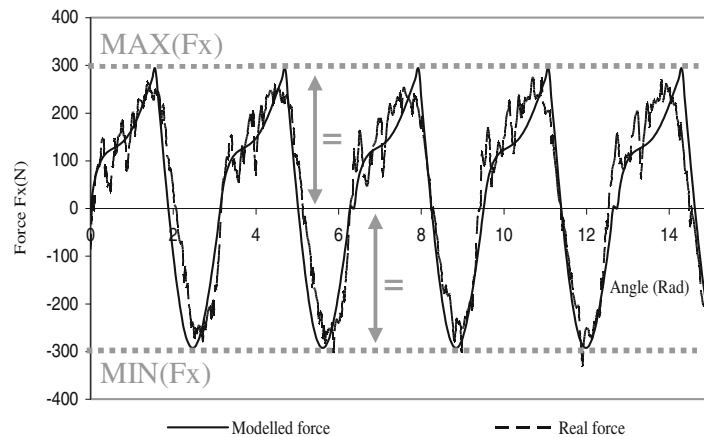
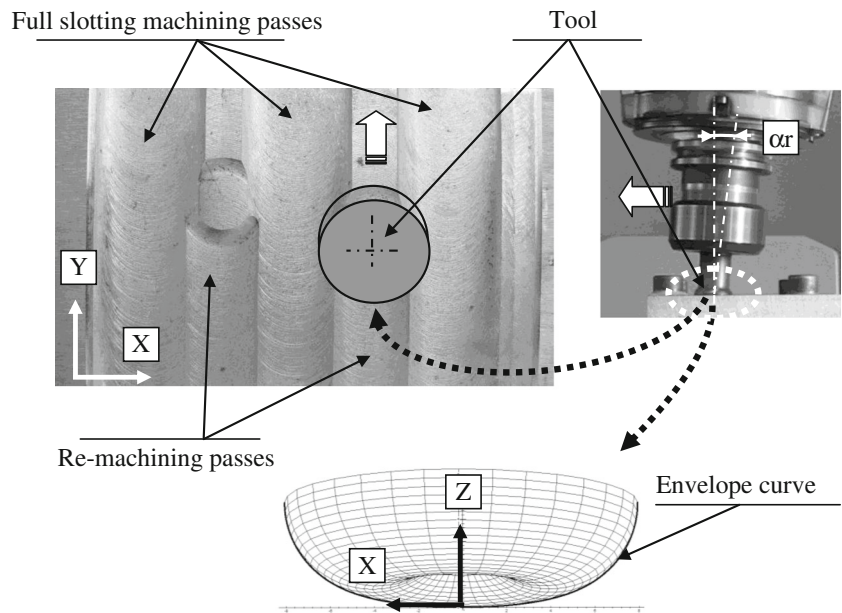


Fig. 9 Re-machining pass and associated envelope curve



$$\alpha_{rinit} / A = B = d_a / 2 \tag{10}$$

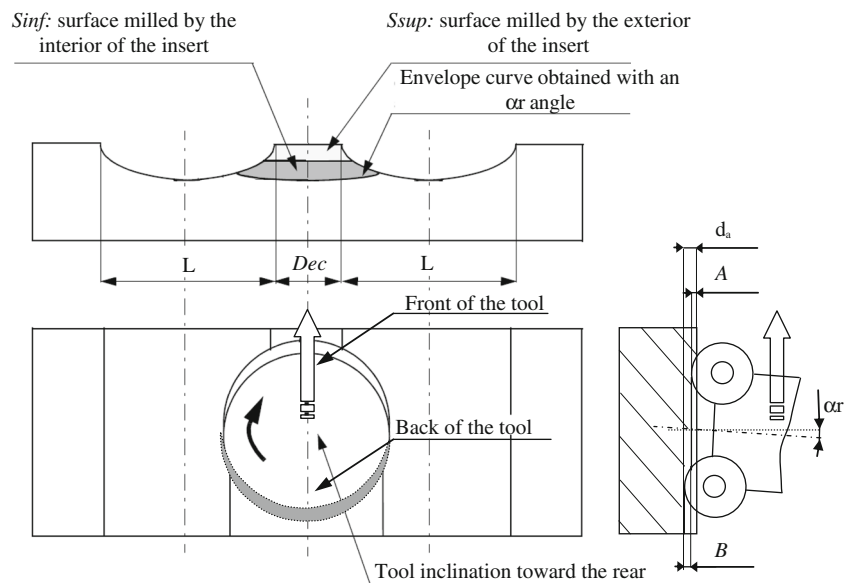
- Second stage: An envelope curve (Fig. 9) is computed using the initial tool axis inclination for recovery toolpaths α_{rinit} . Surfaces S_{inf} and S_{sup} are expressed and weighted by coefficients K_{int} and K_{ext} of the cutting force model presented in Section 2.1.1. The angle α_r is then computed by Eq. 11:

$$\alpha_r / \sin f \times K_{int} = S_{sup} \times K_{ext} \tag{11}$$

This method was applied for a cutter with two teeth ($D = 25$ mm, $R = 5$ mm). The material milled was C35-E (standard

NF EN 10083-1) and the coefficients from the Gilles et al. [11] force model were $K_{int} = 1,550$ MPa, $K_{ext} = 1,470$ MPa, $K_r = 0.35$ and $\nu = -0.2$. The cutting parameters were $d_a = 2$ mm and $f_i = 0.2$ mm with a cutting speed of 140 m/min. In these conditions, the balance angle for full slotting is $\alpha_{eq} = -4.673^\circ$. The width to rework $Dec = 6$ mm was chosen arbitrarily (Fig. 10). The balance angle $\alpha_r = -2.899^\circ$ corresponding to that configuration was computed using the Maple 32 program. The transversal force F_x was constructed for the two-teeth cutter considered, and its theoretical curve can be plotted for the cutting parameters used. In addition, an experiment in the corresponding operating conditions was conducted. Before the re-machining pass, two full slotting machining passes were performed using a balance angle of $\alpha_{eq} = -4.673^\circ$ spacing them

Fig. 10 Breakdown of the machined zone during re-machining pass



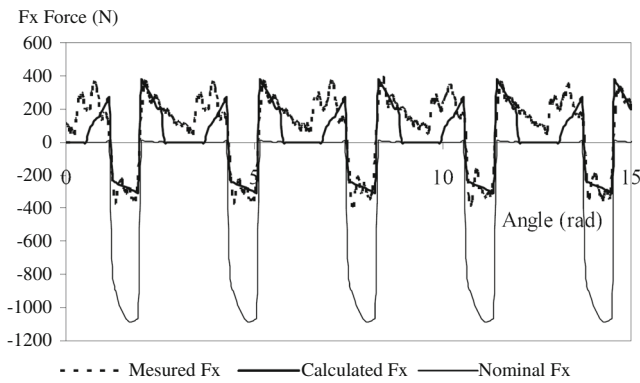


Fig. 11 Experimental validation of tool axis inclination for recovery toolpaths

out by 27.939 mm to obtain the chosen offset $Dec=6$ mm. Figure 11 shows the force modelled by the proposed method, the force measured and the nominal force that is the force obtained for flat machining without using the ploughing angle (for $\alpha r=0$).

Conclusion on balance of transversal cutting force for re-machining passes

- The force measured is consistent with the computed force.
- The cutting entry and exit angle values are consistent as no angular offset is visible on the curves of Fig. 11.
- The amplitude of the F_x nominal force calculated for machining without ploughing angle (for $\alpha r=0$) is 1,088 N while the balanced force has an amplitude of 669 N. This means a reduction of 39 % enabling the sought improvement in the cutter's dynamic behaviour to be achieved.
- The computation method for the balance angle for re-machining passes is thus validated.

2.2 Machining strategy principle

To obtain finished surfaces that comply with their initial specifications, the machining strategy using balancing of the

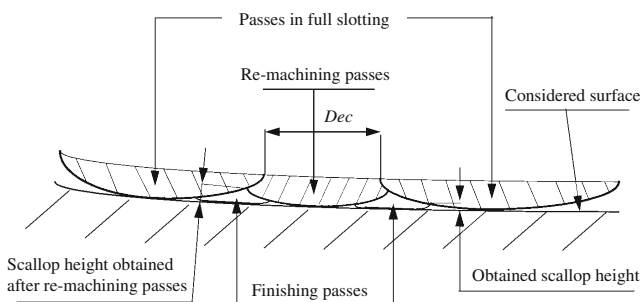


Fig. 12 Different types of passes

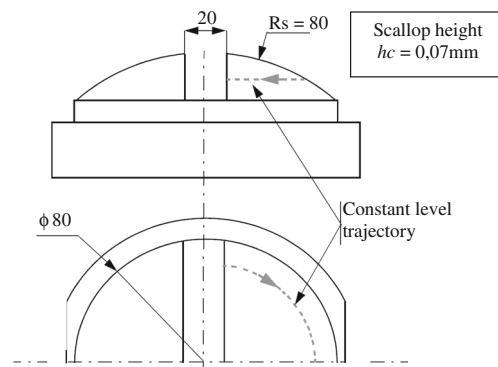


Fig. 13 Spherical dome studied

transversal force will incorporate three types of milling passes (Fig. 12):

- Passes in full slotting performed first and using the transversal cutting force balance angle α_{eq} (Eq. 8): Their spacing will be computed below.
- Re-machining passes located between the full slotting passes: These passes can remove a considerable quantity of material, and it is therefore necessary to calculate a balance angle using the method given in Section 2.1.2.
- Finishing passes, positioned between the full slotting passes and re-machining passes to obtain the specified scallop height: They will only remove a small quantity of material and balancing is therefore not required.

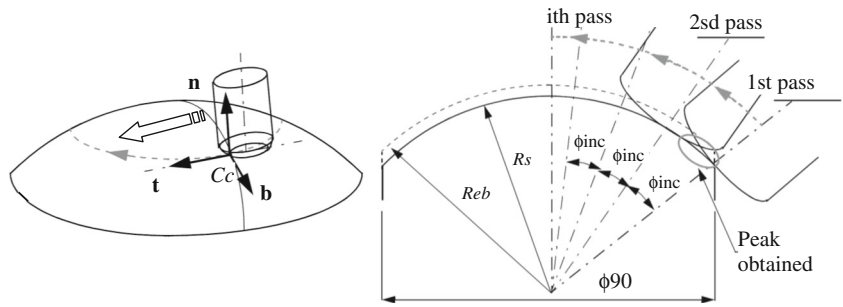
2.3 Strategy associated with balance of the transversal cutting force

The problem posed involves spacing out the passes in full slotting, re-machining passes and finishing passes (Fig. 12) so as to obtain the specified scallop height h_c . The planning flowchart (Fig. 18) authorises two outcomes corresponding to the following cases of machining:

- Machining with full slotting passes and re-machining pass
- Machining with full slotting passes, re-machining pass and finishing passes

Consider a surface (Fig. 12) on which two full slotting passes have been made with the balance angle; the width of material between these two passes is characterised by parameter Dec to which corresponds a balance angle αr of the re-machining pass computed previously. The parameter Dec is initialised at the cutter outer diameter value, and the envelope curves and scallop height are calculated. The parameter Dec is reduced and the various computations iterated until the specified scallop height h_c is reached. If the parameter Dec becomes null without the scallop height h_c being obtained, finishing passes will have to be added. The value of parameter Dec is

Fig. 14 Planning tool paths for the iso-scallop strategy



thus reinitialised to the cutter outer diameter to start up a second full computation loop with finishing passes. The entire strategy as just described is shown in flowchart (Fig. 18).

3 Experimental validation of the method

In this section, the balance of the transversal cutting force strategy is compared with the “iso-scallop” strategy commonly used in five-axis milling. To this purpose, a spherical dome

(Fig. 13) milled at constant levels is chosen as representing a free-form surface with regular geometry for which there is no interference. The various calculations are implemented on a dome arc. The cutter used (Fig. 2) is a torus milling cutter with two teeth ($D=16\text{ mm}$, $R=4\text{ mm}$). The cutting parameters are $d_a=2\text{ mm}$, $f_t=0.2\text{ mm}$ and a cutting speed of 140 m/min . The spherical shape of the workpiece leads to a variation in depth of pass (Fig. 15) under the cutter by just 14 %, allowing the balance angle calculated for machining in full slotting $\alpha_{eq}=-9^\circ$ to be used.

Fig. 15 Planning tool paths for the balance of transversal cutting force strategy

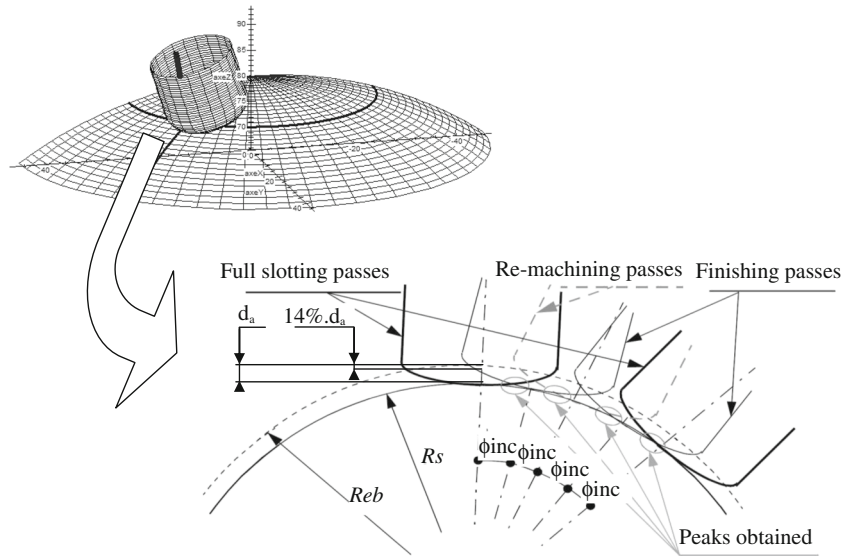


Fig. 16 Scheduling the different passes

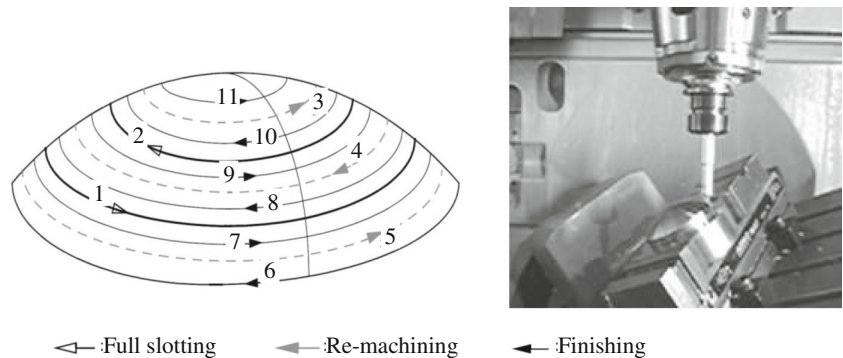


Fig. 17 Execution of two types of milling on the same workpiece

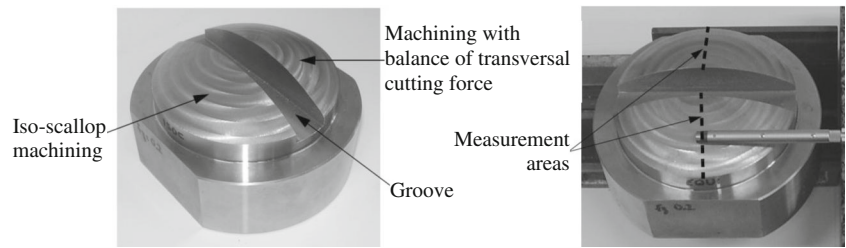


Fig. 18 Toolpath planning flowchart

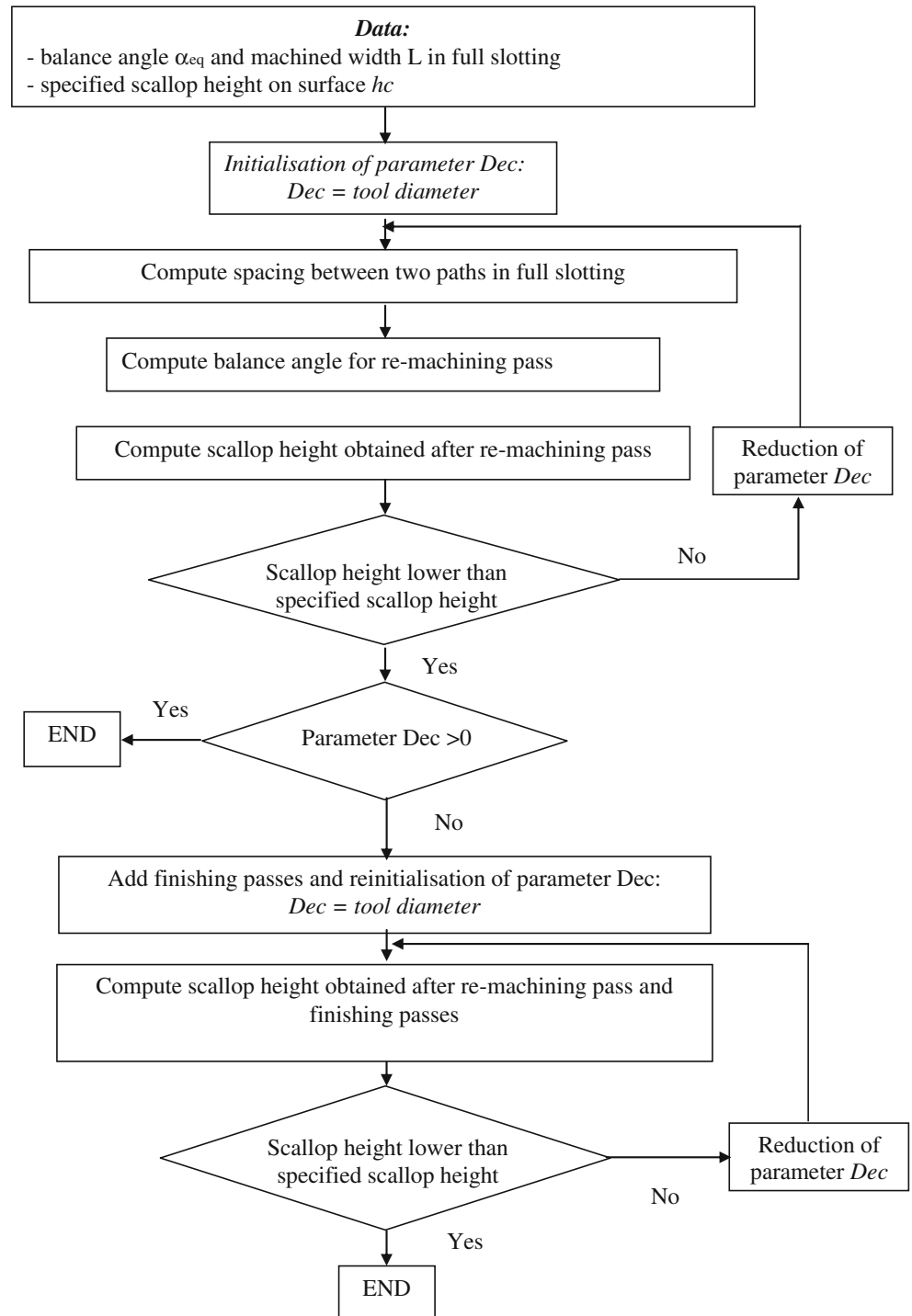


Table 1 Results obtained after machining

Toolpath number	Iso-scallop machining								
	1	2	3	4	5	6	–	–	–
Measure 1	10.05	10.7	12.13	9.56	12.04	7.85	–	–	–
Measure 2	10.25	10.95	12.08	9.45	11.78	7.64	–	–	–
Measure 3	10.11	10.85	12.16	9.61	11.68	7.97	–	–	–
Wt (µm)	10.14	10.83	12.13	9.5	11.83	7.82			
Toolpath number	Machining with balance of transversal cutting force								
	1	2	3	4	5	6	7	8	9
Measure 1	7.35	7.72	7.17	9.32	10.93	10.36	8.16	5.21	5.51
Measure 2	6.95	7.81	7.48	9.07	11.17	10.72	8.45	4.13	5.38
Measure 3	7.04	7.48	7.41	8.93	11.23	10.52	8.52	4.65	5.55
Wt (µm)	7.11	7.67	7.35	9.1	11.1	10.53	8.38	4.99	5.48

3.1 Iso-scallop strategy

In the positioning adopted for iso-scallop machining, the tool-workpiece point of contact is located in front of the cutter (Fig. 14). Furthermore, as this milling does not lead to interference, positioning involves bringing in and orienting the cutter at the point considered on the surface. A first milling pass is set up on the exterior of the workpiece. The second pass is calculated such that the scallop height is equal to the specified scallop height h_c . The third pass is calculated in relation to the second on the same principle and so on. Tool path planning thus comes down to calculating the angular increment ϕ_{inc} shown on Fig. 14 to respect the scallop height criterion. From the machining direction point of view, the workpiece is subjected to climb milling. There is thus only one path direction and a return trip is required between each pass to reposition the cutter. In this case, six passes are necessary to cover the surface.

3.2 “Balance of transversal cutting force” strategy

To replace the parameter Dec (Fig. 12), parameter ϕ_{inc} illustrated in Fig. 15 is used. To apply the method adopted (Fig. 18), two full slotting passes are positioned (Fig. 15) on the dome with angular spacing $2 \times \phi_{inc}$ and a re-machining pass is introduced between them. In accordance with the first loop in the flowchart (Fig. 18), the increment is gradually reduced to obtain the scallop height h_c . The smallest scallop height it is possible to obtain in this instance is 0.205 mm with a tool axis inclination for recovery toolpaths $\alpha_r = -5.766^\circ$

calculated using the method developed in Section 2.1.2. It is thus impossible to mill the surface and respect the scallop height criterion by just using full slotting and re-machining passes. Finishing passes are needed and planning is to be performed using a second loop in the flowchart (Fig. 18).

The computed planning includes two passes in full slotting, three re-machining passes and six finishing passes. The corresponding angular increment is $\phi_{inc} = 3.25^\circ$ and the calculated scallop height 0.064; the criterion $h_c = 0.07$ is thus respected. The tool paths do not require a particular direction and the passes are sequenced in the form of successive to and fro movements (Fig. 16): full slotting passes 1 and 2 correspond to a to and fro movement starting from the exterior of the workpiece towards the interior, while re-machining passes 3, 4 and 5 correspond to a to and fro and a single outward movement from the interior of the workpiece to the exterior. Finally, the finishing passes 6 to 11 correspond to three to and fro movements from the exterior of the workpiece to the interior.

3.3 Comparison between the two methods

The spherical dome is divided into two by a groove (Fig. 17) and iso-scallop machining and machining with balance of transversal cutting force are performed consecutively and without either dismounting the workpiece or cutter replacement on either of the parts. Both machining operations are performed in identical conditions and can thus be compared (Fig. 18).

The set of tool paths was calculated to cover the entire spherical dome, but in practice, the presence of the groove that

Table 2 Comparison of the results obtained after machining

Strategy	Machining time (min, s)	Wt (µm)	Variation
Iso-scallop machining	1 min, 32 s	10.38	0
Machining with balance of transversal cutting force	1 min, 30 s	7.97	-23 %

divides it into two removes passes. There are therefore only six for iso-scallop machining and nine for balanced machining. As the finishing passes present in the balance of transversal cutting force strategy only remove a very small quantity of material, the feed rate f_t is increased to 0.3 mm (instead of 0.2 mm).

To observe the surface quality obtained, the waviness criterion W_t was measured (standard NF EN ISO 4287). Measurements were made using a Surtronic 3+ roughness meter and the TalyProfile 1-2-0 software. The length for evaluation used was 4 mm and the cut-off was 0.8. On both portions of the dome, measurements were made in the same zone remote from cutting entries and exits (Fig. 17). Three measurements of the waviness criterion W_t were noted on each pass and a mean was then computed (Table 1). Despite a higher number of passes for the balance of transversal cutting force strategy, the machining times remained comparable as the feed rate used for the finishing passes was increased to $f_t=0.3$ mm. A mean was calculated in order to compare the results obtained with the two strategies. These results are shown in Table 2.

3.4 Discussion of results

The most effective milling in terms of surface quality was performed using the balance of transversal cutting force strategy; this thus validates the proposed method that makes for a 23 % enhancement on the waviness criterion W_t as compared with the iso-scallop method generally used to machine free-form surfaces in five-axis milling. This improvement in surface quality that derives from the dynamic behaviour of the cutter will be all the more significant in so far as the cutter is deformable, this being the case for long, fine cutters used to work mould cavities or aeronautical fittings. For such workpieces, the improvement obtained will thus be distinctly better by 23 %. In addition, this improvement in mean roughness represents a major advantage for tools that then have to go on to a polishing stage.

4 Conclusion

The machining strategy that has been presented above uses the balance of transversal cutting force criterion together with cutter positioning combined with five-axis milling in order to obtain an improvement in surface quality. Its principle involves implementing a distribution of different passes (full slotting, re-machining and finishing) so as to manage the scallop height criterion. This method means finished surfaces of better quality can be obtained than those produced using the iso-scallop method generally used. The improvement obtained means the polishing time required for moulds and matrices can be optimised, and manufacturing time as a whole

can be reduced through increasing the feed rate in so far as a constant level of surface quality can be maintained.

Another aspect of the present method is that it improves the dynamic behaviour of the cutter (as already recounted in previous works [12, 13]). Indeed, using cutter ploughing effects leads to those cutters being stabilised during machining, thanks to much smoother cutting entries and exits. The global stress on the cutter is thus reduced and its dynamic behaviour improved. The findings described here show how this improvement in dynamic behaviour contributes to a gain in surface quality. Work is now in progress for a further publication to explain the special cutting mechanism of a cutter in a ploughing situation and how that mechanism tends to smooth out the stresses sustained by the cutter and increase its lifetime.

References

1. Kruth JP, Klewais P (1994) Optimization and dynamic adaptation of the cutter inclination during five-axis milling of sculptured surfaces. *Ann CIRP* 43(1):443–448
2. Jensen CG, Red WE, Pi J (2002) Tool selection for five-axis curvature matched machining. *Comput Aided Des* 34(3):251–266
3. Krzysztof M (1987) Influence of surface shape on admissible tool positions in 5-axis face milling. *Comput Aided Des* 19(5):233–236
4. Chen T, Ye P, Wang J (2005) Local interference detection and avoidance in five-axis NC machining of sculptured surfaces. *Int J Adv Manuf Technol* 25(3–4):343–349
5. Yuan-Shin L (1997) Admissible tool orientation control of gouging avoidance for 5-axis complex surface machining. *Comput Aided Des* 29(7):507–521
6. Jianhua F, Alan B (2008) Quadric method for cutter orientation in five-axis sculptured surface machining. *Int J Mach Tool Manuf* 48(7–8):788–801
7. Warkentin A, Ismail F, Bedi S (2000) Multi-point tool positioning strategy for 5-axis machining of sculptured surfaces. *Comput Aided Geom Des* 17(1):83–100
8. Gray PJ, Bedi S, Ismail F (2005) Arc-intersect method for 5-axis tool positioning. *Comput Aided Des* 37(7):663–674
9. Rubio W (1993) *Génération de trajectoires du centre de l'outil pour l'usinage de surfaces complexes sur machines à trois et cinq axes*. Thèse de doctorat, Université Paul Sabatier, Toulouse III
10. Patrick G, Frederic M, Walter R (2006) Modelling cutting forces in milling on torus cutters. *Int J Mach Mach Mater* 1:166–185, N°2
11. Gilles P, Monies F, Rubio W (2007) Optimum orientation of a torus milling cutter: method to balance the transversal cutting force. *Int J Mach Tool Manuf* 47(15):2263–2272
12. Gilles P, Cohen G, Monies F, Rubio W (2009) Dynamic behaviour improvement for a torus milling cutter using balance of the transversal cutting force. *Int J Adv Manuf Technol* 40(7–8):669–675
13. Gilles P, Cohen G, Monies F, Rubio W (2013) Torus cutter positioning in five-axis milling using balance of the transversal cutting force. *Int J Adv Manuf Technol* 66(5–8):965–973
14. Redonnet J-M, Rubio W, Monies F, Dessein G (2000) Optimising tool positioning for end-mill machining of free-form surfaces on 5-axis machines for both semi-finishing and finishing. *Int J Adv Manuf Technol* 16(6):383–391

15. Monies F, Mousseigne M, Redonnet J-M, Rubio W (2004) Determining a collision-free domain for the tool in five axis machining. *Int J Prod Res* 42(21):4513–4530
16. Gilles P, Senatore J, Segonds S, Monies F, Rubio W (2012) Determination of angular fields outside low and high collisions to mill free-form surfaces on 5-axis CNC machines. *Int J Prod Res* 50(4):1045–1061
17. Chiou C-J, Lee Y-S (1999) A shape-generating approach for multi-axis machining G-buffer models. *Comput Aided Des* 31(12): 761–776